Chinese Chemical Letters 32 (2021) 2127–2138

Contents lists available at ScienceDirect

Chinese Chemical Letters

journal homepage: www.elsevier.com/locate/cclet

Review

Hydrogen peroxide-generating nanomedicine for enhanced chemodynamic therapy

Peng Yu[a], Xiaodong Li[c], Guohui Cheng[a], Xu Zhang[a], Dan Wu[b,*], Jin Chang[a,*], Sheng Wang[a,*]

[a] School of Life Sciences, Tianjin University, Tianjin 300072, China
[b] College of Chemical and Biological Engineering, Zhejiang University of Technology, Hangzhou 310014, China
[c] The Second Hospital, Tianjin Medical University, Tianjin 300211, China

ARTICLE INFO

Article history:
Received 2 November 2020
Received in revised form 8 February 2021
Accepted 9 February 2021
Available online 11 February 2021

Keywords:
Nanomedicine
ROS
Chemodynamic therapy
Fenton reaction
Hydrogen peroxide

ABSTRACT

Chemodynamic therapy (CDT) is an emerging endogenous stimulation activated tumor treatment approach that exploiting iron-containing nanomedicine as catalyst to convert hydrogen peroxide (H_2O_2) into toxic hydroxyl radical ($^{\bullet}OH$) through Fenton reaction. Due to the unique characteristics (weak acidity and the high H_2O_2 level) of the tumor microenvironment, CDT has advantages of high selectivity and low side effect. However, as an important substrate of Fenton reaction, the endogenous H_2O_2 in tumor is still insufficient, which may be an important factor limiting the efficacy of CDT. In order to optimize CDT, various H_2O_2-generating nanomedicines that can promote the production of H_2O_2 in tumor have been designed and developed for enhanced CDT. In this review, we summarize recently developed nanomedicines based on catalytic enzymes, nanozymes, drugs, metal peroxides and bacteria. Finally, the challenges and possible development directions for further enhancing CDT are prospected.

1. Introduction

Reactive oxygen species (ROS), such as superoxide anion (O_2^-), hydrogen peroxide (H_2O_2) and hydroxyl radical ($^{\bullet}OH$), generally refer to a class of highly active reduction products of oxygen with one or more unpaired electrons [1]. Normal body metabolism produces part of ROS, and ROS at normal concentration are beneficial to cell growth and proliferation [2]. However, high level of ROS will damage nucleic acids and proteins, which is detrimental to cell survival. Furthermore, cancer cells often lack some key antioxidant enzymes, so they are more susceptible to damage by increased intracellular ROS concentration [3]. Take advantage of this characteristic of cancer cells, various ROS-based treatment approaches that kill cancer cells by further promoting the generation of ROS at tumor sites have received increasing attention in recent years [4–8]. This treatment strategy based on the different responses of cancer cells and normal cells to ROS has brought relatively specific tumor targeting and protection to normal cells.

Among the ROS generation approaches, iron-mediated Fenton reaction is a promising method that converts less-reactive H_2O_2 into highly toxic $^{\bullet}OH$ in acidic condition [9]. Based on Fenton reaction, chemodynamic therapy (CDT), which uses iron-containing nanomedicine as catalyst to generate toxic $^{\bullet}OH$ at the tumor site, has attracted much attention in recent years [10,11]. The amount of ROS production is critical in ROS-based treatment strategies because insufficient amount of ROS can even promote the development of the tumor [12]. In general, H_2O_2 is overexpressed in weak acidic tumor microenvironment (TME); while insufficient in weak alkaline normal tissues [13]. The environmental difference between tumor tissue and normal tissue ensures high selectivity and low side effect of CDT [14]. The therapeutic effect of CDT often depends on the strength of Fenton response [15]. Therefore, it is increasingly important to find suitable ways to promote the Fenton response to improve efficacy.

Various methods such as optimizing nanomaterials [16–19], adjusting the reaction environment [20], and introducing external energy [21,22] have been developed for improving Fenton reaction efficacy. However, as an important substrate of the Fenton reaction, the endogenous H_2O_2 in tumor is still insufficient to generate sufficient $^{\bullet}OH$, which may be an important factor limiting the efficacy of CDT. In order to increase the concentration of H_2O_2 in tumor, targeted delivery of exogenous H_2O_2 through nanocarriers

* Corresponding authors.
E-mail addresses: danwu@zjut.edu.cn (D. Wu), jinchang@tju.edu.cn (J. Chang), shengwang@tju.edu.cn (S. Wang).

https://doi.org/10.1016/j.cclet.2021.02.015
1001-8417/

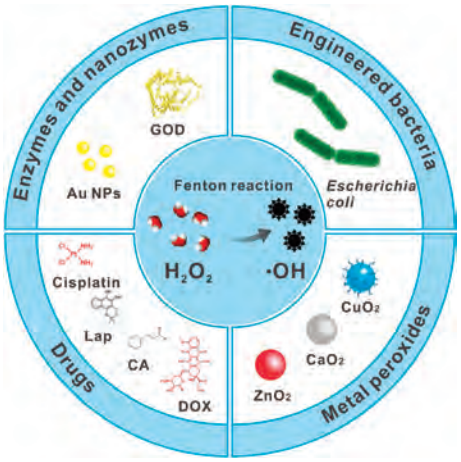

Fig. 1. Schematic illustration of H_2O_2-generating nanomedicines for enhanced CDT.

has been studied [23]. But the leakage of H_2O_2 during transportation may cause low delivery efficiency and damage to normal cells. Another method to increase intratumoral H_2O_2 level is promoting the production of H_2O_2 in tumor. In order to ensure the selective production of a large amount of H_2O_2 at the tumor site, various H_2O_2-generating nanomedicines containing catalytic enzymes or nanozymes, drugs, metal peroxides and even bacteria have been designed and developed for enhanced CDT (Fig. 1). Herein, we will briefly introduce the working mechanisms and applications of these nanomedicines (Table 1) [2,24–42]. The prospects and challenges are also discussed.

2. Enzymes and nanozymes

One of the main methods for generating H_2O_2 *in situ* is utilizing catalysis of enzymes, of which the most widely used is glucose oxidase (GOD) [43]. GOD can convert glucose into H_2O_2 and glucose acid in the presence of oxygen, which provides the possibility to solve the hydrogen peroxide deficiency [44]. The large amount of glucose in TME provides favorable conditions for GOD to produce H_2O_2 [45]. And the production of glucose acid further enhances the acidity of TME, which can promote the efficiency of Fenton reaction.

Recently, a large number of studies have reported GOD-mediated production of H_2O_2 for CDT [44]. Lin *et al.* prepared a manganese dioxide (MnO_2)-coated iron carbide (Fe_5C_2) magnetic nanoparticle for GOD loading, the resulted Fe_5C_2-GOD@MnO_2 could be used for CDT through Fenton reaction (Fig. 2a) [27]. In response to the weak acidity of TME, MnO_2 would decompose into Mn^{2+} and O_2, leading to increased O_2 concentration and GOD release. The O_2 can promote the catalytic efficiency of GOD to produce sufficient H_2O_2 in tumor region. Finally, $^{\bullet}OH$ could be generated through Fe_5C_2-mediated Fenton reaction for triggering tumor cells apoptosis and death. As shown in Fig. 2b, in the presence of glucose, the characteristic peaks of $^{\bullet}OH$ were observed in electron spin resonance (ESR) spectrum of the Fe_5C_2-GOD@-MnO_2, indicated that $^{\bullet}OH$ was generated in this situation. However, no obvious signals were detected without glucose, indicating the key role of glucose in $^{\bullet}OH$ generation. The generation of $^{\bullet}OH$ in different conditions were further quantitatively analyzed by chromogenic 1,3-diphenylisobenzofuran (DPBF), which can be oxidized by $^{\bullet}OH$ into colorless radicals. As shown in Fig. 2c, under acidic condition with glucose, the absorbance of DPBF was decreased obviously, indicating a large amount of $^{\bullet}OH$ was generated; in contrast, under neutral conditions or acidic condition without glucose, the absorbance of DPBF did not decrease significantly. These results demonstrated that GOD-mediated H_2O_2 producing can effective enhance the $^{\bullet}OH$ generation. The intracellular ROS was detected by using a ROS probe, 2′,7′-dichlorofluorescin diacetate (DCFH-DA). As shown in Figs. 2d and e, cells incubated with Fe_5C_2@MnO_2 did not show intracellular ROS level change when compared with control group, indicated that the GOD was the critical part in ROS generation process. *In vitro* cell viability and live/dead cell staining results proved that Fe_5C_2@MnO_2 has good biocompatibility and negligible cytotoxicity; while Fe_5C_2-GOD@MnO_2 exhibited strong inhibitory activity on HeLa cells (Figs. 2f and g). Furthermore, the therapy effect could be improved by magnetic targeting. The anticancer effect of Fe_5C_2-GOD@MnO_2 was further demonstrated by *in vivo* experiment. The tumor growth was significantly inhibited by Fe_5C_2-GOD@MnO_2, indicating the effectiveness of CDT. Importantly, magnetic targeted Fe_5C_2-GOD@MnO_2 group displayed the best antitumor efficacy with the inhibition rate of 92% (Fig. 2h). Therefore, the nanocatalytic particles have the characteristics of magnetic targeting, TME response, high safety, and strong anti-cancer effect.

In addition, GOD has been combined with a variety of Fe-containing nanomaterials including ultra-small Fe_3O_4 nanoparticles and metal–organic frameworks for H_2O_2 production-enhanced CDT [24,26]. However, as a natural protein, GOD suffers from the disadvantages of immunogenicity, high cost and short half-life *in vivo* [44]. These shortcomings severely hinder its bioapplications. Recently, alternatives to natural enzymes, catalytically active nanomaterials, which are often called "artificial enzymes" or "nanozymes", have become more and more attractive due to their advantages of easy manufacturing, low cost, and strong adaptability [46]. Nowadays, a large number of mimetic enzymes have been developed. For example, ultra-small gold (Au) nanoparticles (NPs) have been demonstrated to have catalytic properties similar to GOD. In the presence of dissolved oxygen, ultra-small Au NPs can oxidize glucose into glucose acid and H_2O_2, which is fully in line with the characteristics of GOD substitutes [47]. Shi *et al.* reported a dual inorganic nanozyme system for efficient tumor CDT [28]. As sown in Fig. 3a, ultra-small Au NPs and iron oxide (Fe_3O_4) NPs were dispersed in the pores of dendritic

Table 1
A summary of various methods to increase H_2O_2 level.

Classify	Specific substance	Mechanism of generating H_2O_2	Other necessary substances	Ref.
Enzymes and nanozymes	Glucose oxidase	Catalysis	Glucose, O_2	[24–27]
	Au nanoparticles	Catalysis	Glucose, O_2	[28]
Drugs	Platinum drugs	Activation of related enzyme	NOX, O_2	[29–31]
	Doxorubicin	Catalysis	NOX, O_2	[32,33]
	β-Lapachone	Catalysis	NQO1, O_2	[34,35]
	Cinnamaldehyde	Catalysis	O_2	[2,36,37]
Metal peroxides	Calcium peroxide	Self-supply	H^+	[38,39]
	Copper peroxide	Self-supply	H^+	[40]
	Zinc peroxide	Self-supply	H^+	[41]
Engineered bacteria	*Escherichia coli*	Expression of related enzymes	O_2	[42]

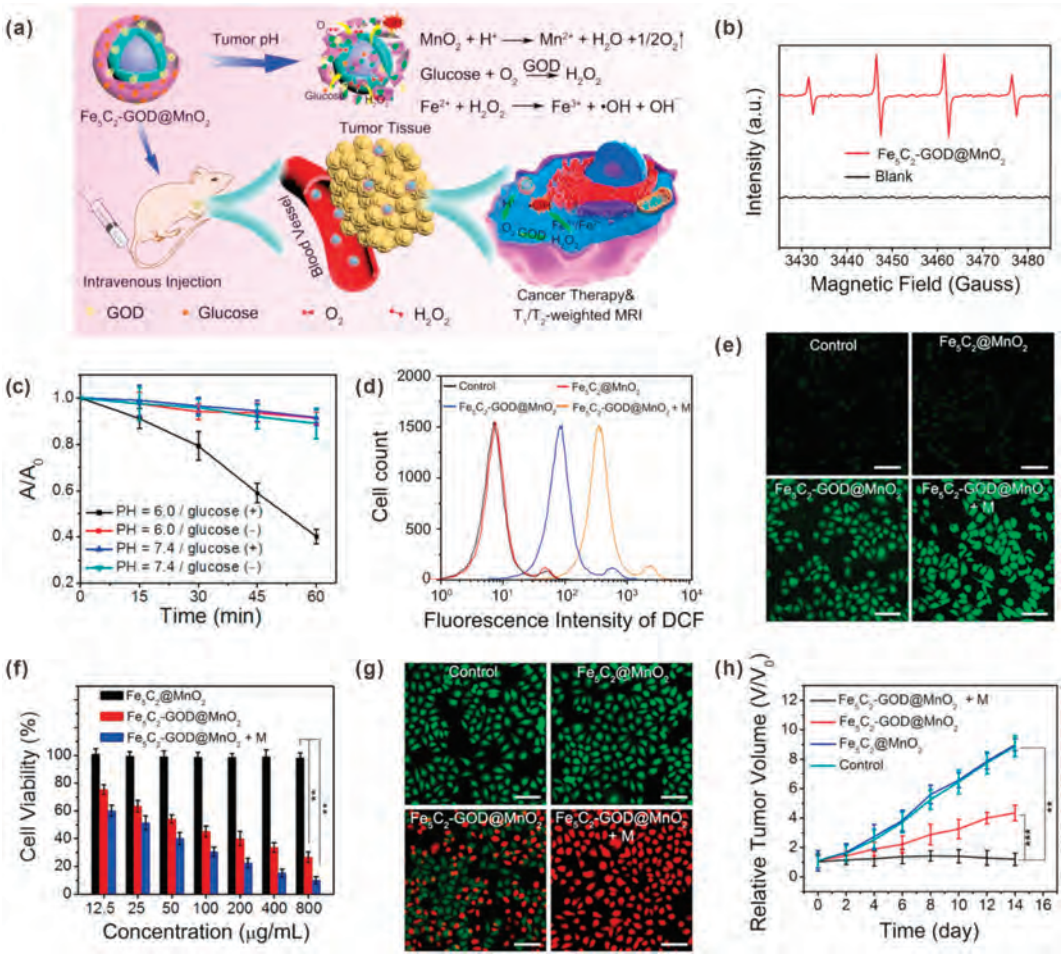

Fig. 2. (a) Schematic illustration of Fe_5C_2-GOD@MnO_2 nanocatalysts for H_2O_2 generation-enhanced CDT. (b) ESR spectra of Fe_5C_2-GOD@MnO_2 in the presence and absence of glucose (10 mmol/L) at pH 6.0. (c) Normalized absorption changes of DPBF after incubation with Fe_5C_2-GOD@MnO_2 at different pH. (d) Flow cytometry analysis of DCFH-DA stained HeLa cells with different treatments. (e) Fluorescence images of DCFH-DA stained HeLa cells with different treatments. (f) Viability of HeLa cells upon different treatments. (g) Live/dead cell staining results of HeLa cells with different treatments. (h) Relative tumor volume of mice after different treatments. Reproduced with permission [27]. Copyright 2018, American Chemical Society.

mesoporous silica NPs (DMSN). After surface poly(ethylene glycol) (PEG) modification, the resulting nanozyme system (DMSN-Au-Fe_3O_4-PEG) without any toxic substances was obtained. The Au NPs can be used as a GOD mimic to catalyze H_2O_2 generation (process I); while Fe_3O_4 NPs can be used as a peroxidase mimic to catalyze $^{\bullet}OH$ generation (process II). To demonstrate the function of Au NPs, a colorimetric assay was performed to detect gluconic acid, which is a typical product of glucose oxidation reaction. As shown in Fig. 3b, the absorbance of DMSN-Au NPs solution increased with increasing glucose concentration, indicated that gluconic acid was produced through Au NPs-catalyzed reaction. In addition, with the process of reaction, the oxygen level of the solution containing DMSN-Au decreased rapidly, confirming oxygen consumption during catalytic process (Fig. 3c). These results confirmed that Au NPs have the GOD mimic function of catalyzing the production of H_2O_2 from glucose. Then 3,3′,5,5′-tetramethylbenzidine (TMB) colorimetric assay was used to confirm $^{\bullet}OH$ generation in process II. In the presence of DMSN-Au-Fe_3O_4 and glucose, absorption peaks were observed, indicating the cascade catalytic effects of DMSN-Au-Fe_3O_4 (Fig. 3d). The $^{\bullet}OH$ generation was also evaluated in 4T1 cells by using DCFH-DA. Strong green fluorescence was observed inside cells incubated with glucose and DMSN-Au-Fe_3O_4, demonstrated that the DCFH-DA was oxidized into fluorescent 2′,7′-dichlorofluorescein (DCF) by generated $^{\bullet}OH$ (Fig. 3e). Based on the efficient cascade catalysis of Au NPs and Fe_3O_4 NPs, the DMSN-Au-Fe_3O_4 showed great tumor-growth inhibition effect (Fig. 3f). It should be noted that the GOD-like activity of Au NPs was affected by many factors, such as size, shape, surface chemistry, concentration and environmental pH value. For example, the catalytic activity of Au NPs could be blocked by surface modification. Furthermore, it has been reported that Au nanorods (and other metals including Ag, Pd and Pt) also have intrinsic peroxidase-like and catalase-like activities. Under acidic and neutral conditions, Au nanorods mainly exerted peroxidase-like activity; while under alkaline condition they exerted catalase-like activity [48]. Therefore, in the development and application of nanozymes, their physical and chemical properties and application environment of nanozyme should be considered. In addition, the GOD- and nanozyme-mediated H_2O_2 generation is an oxygen-consuming process; therefore, improving the hypoxia of tumor microenvironment may be beneficial to the performance of these enzymes and nanozymes [49].

In another study, Qu *et al.* designed a nanozyme that can promote the effective accumulation of H_2O_2 at the tumor site by perturbing H_2O_2 balance [50]. The nanozyme (PZIF67-AT) was composed of metal–organic framework (ZIF-67) and inhibitor 3-amino-1,2,4-triazole (AT). The PZIF67-AT had superoxide dismutase-like activity, which can promote the production of H_2O_2.

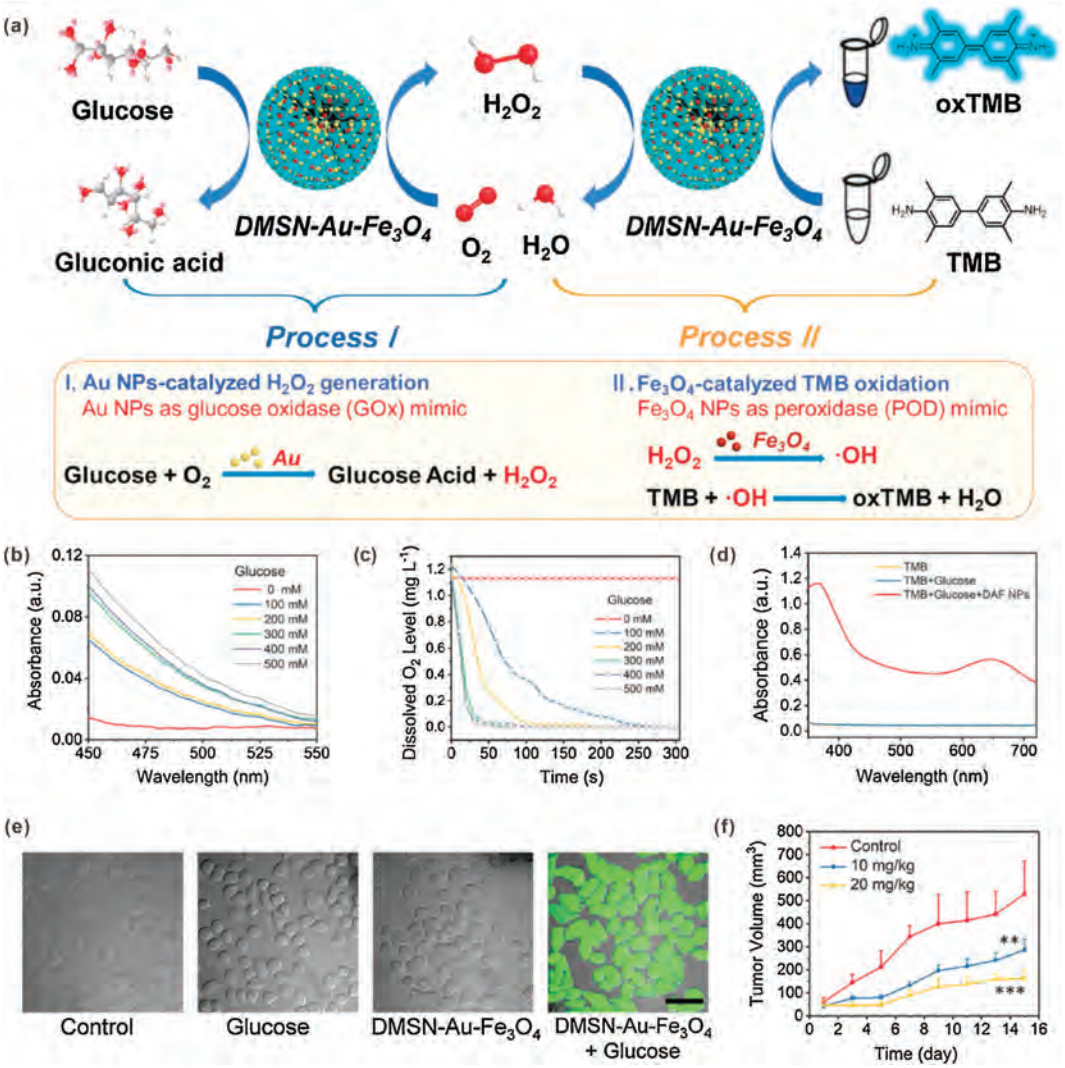

Fig. 3. (a) Schematic illustration of DMSN-Au-Fe_3O_4 nanoplatform for $^{\bullet}OH$ generation by two reaction processes. (b) Absorption spectra of DMSN-Au solutions incubated with different concentrations of glucose in the presence of hydroxylamine and $FeCl_3$. (c) Oxygen level changes of DMSN-Au solutions incubated with different concentrations of glucose. (d) Absorption spectra of TMB after different treatments at pH 6.5. (e) Fluorescence imaging of DCFH-DA stained 4T1 cells after different treatments. (f) Tumor growth curves of mice after different treatments. Reproduced with permission [28]. Copyright 2019, Wiley-VCH.

Meanwhile, the loaded AT can inhibit activity of catalase, resulting in decreased H_2O_2 decomposition. Therefore, the nanozyme could effectively promote the accumulation of H_2O_2. In addition, the PZIF67-AT can further convert H_2O_2 into $^{\bullet}OH$ through Fenton-like reaction to realize efficient CDT.

3. Drugs

Besides enzymes and nanozymes, various chemotherapeutic drugs such as platinum drugs, doxorubicin (DOX), cinnamaldehyde (CA) and β-lapachone (Lap) have been used to promote the production of H_2O_2.

Cisplatin is not only the first metal-based chemotherapy drug, but also one of the most effective chemotherapy drugs [51]. A large number of experiments have proved that cisplatin has a good inhibitory effect on a variety of tumors, making it a representative of chemotherapy drugs. The nature of cisplatin that can induce the generation of ROS has attracted much attention [52]. Specifically, cisplatin activates a family of enzymes called nicotinamide adenine dinucleotide phosphate (NADPH) oxidase (NOX) in cancer cells [53]. The activated NOX can catalyze NADPH to $NADP^+$, and at the same time give an electron to O_2 to convert it into O_2^- [54], and then disproportionate by superoxide dismutase (SOD) to produce H_2O_2. Therefore, due to the characteristic of cisplatin to promote the generation of H_2O_2, the combination of cisplatin chemotherapy and CDT has become a promising approach, which can reduce the toxic and side effects of cisplatin and improve the efficacy. For example, Mao *et al.* constructed an organic nano-drug (PTCG NPs) by using epigallocatechin-3-gallate (EGCG), phenolic platinum (IV) prodrug (Pt-OH), ferric chloride and polyphenol-modified block copolymer (PEG-*b*-PPOH) for synergistic chemotherapy and CDT (Fig. 4a) [29]. In response to low pH and glutathione (GSH) environments, the PTCG NPs will be disassembled and Pt-OH will be activated, leading to rapid release of cisplatin (Figs. 4b and c). The released active cisplatin will promote the generation of H_2O_2 through the abovementioned processes. Catalyzed by Fe ions, the $^{\bullet}OH$ will be further generated through Fenton reaction for CDT. The intracellular ROS levels inside cells with different treatments were determined by DCFH-DA. As shown in the confocal laser scanning microscopy (CLSM) images (Fig. 4d), very weak green fluorescence was observed in $FeCl_3$ group, demonstrated that the endogenous H_2O_2 was insufficient for $^{\bullet}OH$ generation. It can be clearly seen that the PTCG NPs-treated HepG2 cells showed the strongest intracellular green fluorescence, indicating the enhancement of ROS

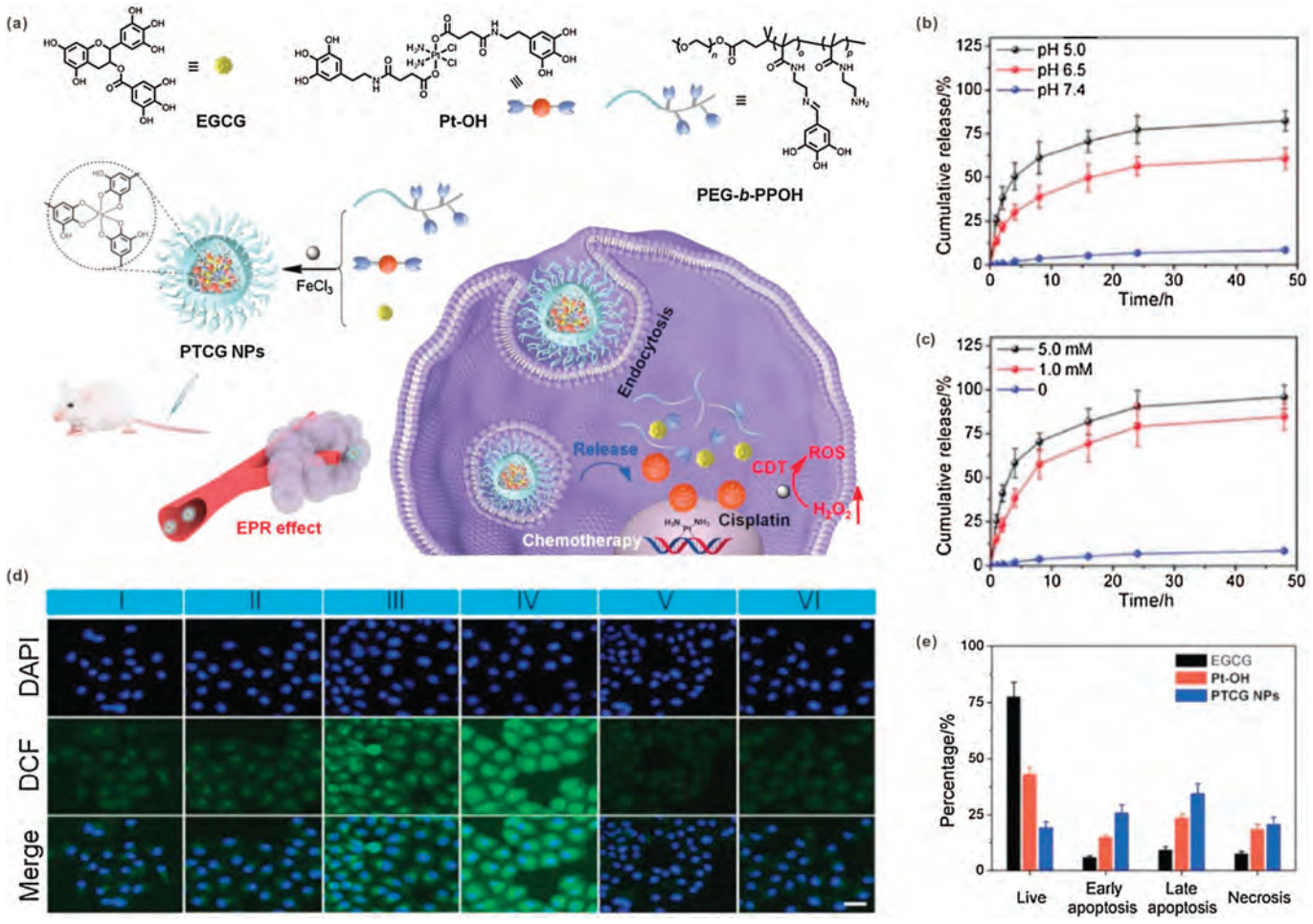

Fig. 4. (a) Schematic illustration of PTCG NPs for synergistic chemotherapy/CDT. (b) *In vitro* platinum release from PTCG NPs at different pH. (c) *In vitro* platinum release from PTCG NPs at different concentrations of GSH (mM: mmol/L). (d) CLSM images of DCFH-DA stained HepG2 cells after different treatments (Goups I-VI: Control; $FeCl_3$; cisplatin + $FeCl_3$; PTCG NPs; PTCG NPs + VC; PTCG NPs + DFO). (e) Cell apoptosis results of HepG2 cells after different treatments. Reproduced with permission [29]. Copyright 2020, Wiley-VCH.

generation. Both vitamin C (VC, ROS scavenger) and deferoxamine mesylate (iron chelator) could block the effect of PTCG NPs, demonstrated that the ROS was generated through an iron-involved reaction. Due to the synergistic effect of chemotherapy and CDT, the HepG2 cells incubated with PTCG NPs showed higher levels of apoptosis and necrosis than that incubated with EGCG or Pt-OH (Fig. 4e). Animal experiments also proved that PTCG NPs had the best inhibitory effect on tumors, and the inhibition rate of PTCG NPs was as high as 81.6%. Owing to the great therapeutic performance and biological safety of PTCG NPs, the survival time of PTCG NPs-treated mice was obviously prolonged.

DOX is a clinical anthracycline drug for treatment of malignant tumor by inhibiting the synthesis of DNA and RNA. Due to the broad-spectrum anti-cancer and good curative effect of DOX, it has been widely used in the treatment of malignant lymphoma, leukemia, prostate cancer and various solid tumors [55]. However, excellent antitumor effect is often accompanied by serious side effects. The strong cardiotoxicity of DOX can cause heart failure [56]. Therefore, the development of combination treatment strategies is highly desirable for optimizing DOX-based therapy [57]. The effect of DOX on the promotion of ROS generation has attracted the attention of researchers [58–60]. The working mechanism of DOX is similar to that of cisplatin. Based on this property of DOX, Sun *et al.* developed a DOX and AT (a catalase inhibitor) co-loaded iron oxide mesoporous silica core–shell NPs (Fe_3O_4@MSN) for chemo/chemodynamic combination therapy [33]. After folate (FA) and triphenylphosphonium (TPP) modification, the DOX/AT@Fe_3O_4@MSN-TPP/PEG-FA can realize cancer cell and mitochondrial targeted therapy. In cancer cells, the released DOX could stimulate the activation of NOXs, converting O_2 into $O_2^{\cdot-}$. Then the production of H_2O_2 was promoted by SOD. Moreover, AT could reduce the decomposition of H_2O_2 through inhibiting catalase activity. By combining the promotion of H_2O_2 production and inhibition of H_2O_2 decomposition, the intracellular H_2O_2 level could be significantly improved for efficient Fenton reaction (Fig. 5a). Quantitative analysis of intracellular ROS by flow cytometry showed that the ROS levels in both breast adenocarcinoma cells (MCF-7) and human gastric carcinoma cells (MGC-803) were obviously improved by the incubation of DOX-containing nanomedicines (Fig. 5d). The addition of Fe_3O_4 can further amplify ROS level, which may attribute to the $^{\cdot}OH$ generation through Fenton reaction. The cytotoxicity results showed that the DOX/AT@Fe_3O_4@MSN-TPP/PEG-FA had a significant inhibitory effect on both MCF-7 and MGC-803 cancer cells, which was stronger than that of other groups (Figs. 5b and c). This result proved that the chemo/CDT combination treatment outcome could be further enhanced by AT. In addition, the induced apoptosis rate of the DOX/AT@Fe_3O_4@MSN-TPP/PEG-FA reached 88.1%, confirming the higher efficacy of the synergistic therapy. The characteristic of this study is not only the combination of chemo/chemodynamic therapy, but also the introduction of multi-level targeting and catalase inhibitors, which improves the targeting while further improving

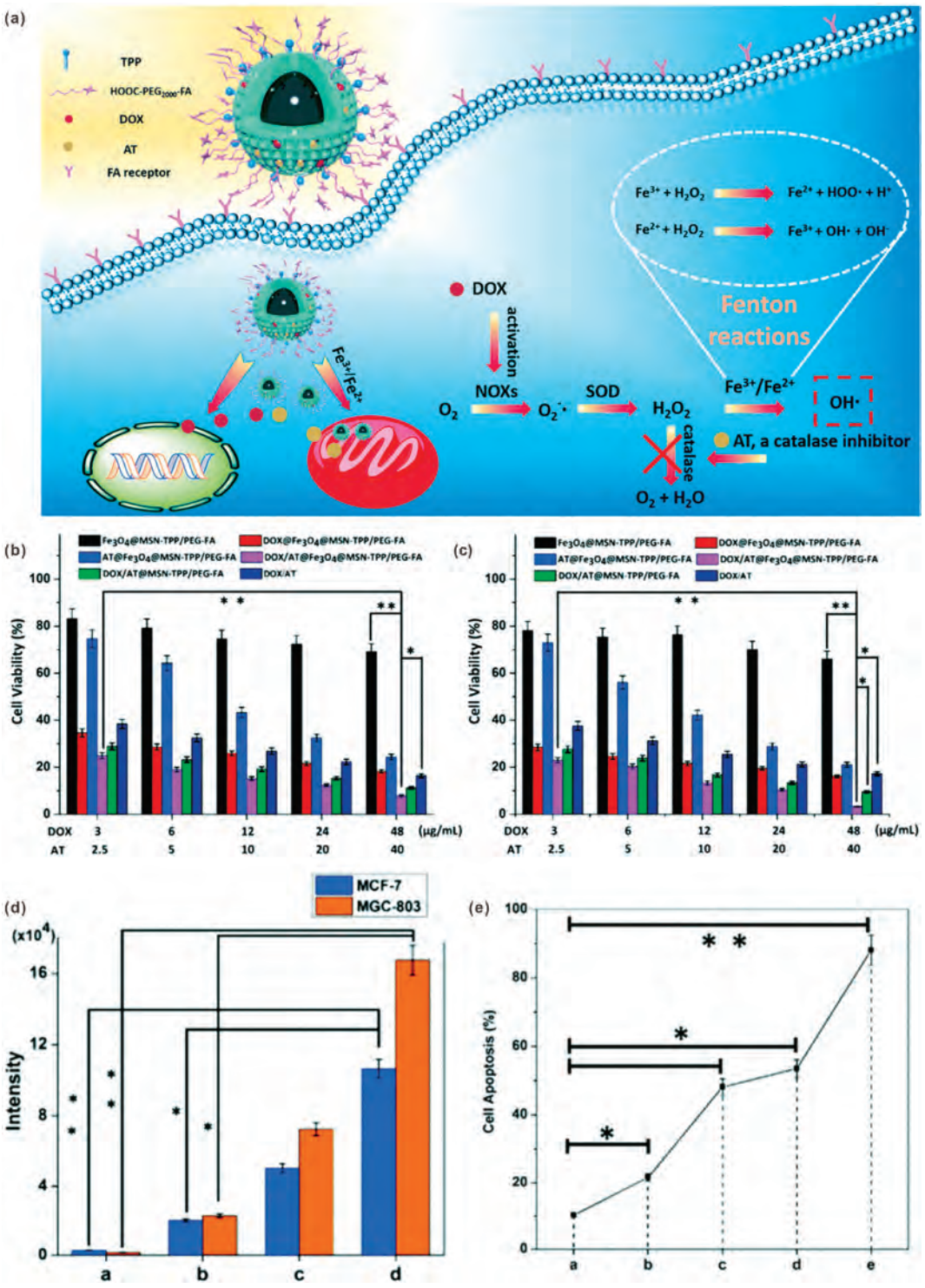

Fig. 5. (a) Schematic illustration of DOX/AT loaded Fe_3O_4@MSN-TPP/PEG-FA for mitochondria-targeted CDT. Viabilities of MCF-7 cells (b) and MGC-803 cells (c) treated with different samples. (d) Intracellular ROS levels detected by DCFH-DA staining and flow cytometry analysis (Groups a-d: control; DOX/AT-loaded MSN-TPP/PEG-FA; DOX/AT-loaded Fe_3O_4@MSN; DOX/AT-loaded Fe_3O_4@MSN-TPP/PEG-FA). (e) Cell apoptosis results of HepG2 cells after different treatments (Groups a-e: Fe_3O_4@MSN-TPP/PEG-FA; AT-loaded Fe_3O_4@MSN-TPP/PEG-FA; DOX-loaded Fe_3O_4@MSN-TPP/PEG-FA; DOX/AT-loaded MSN-TPP/PEG-FA; DOX/AT-loaded Fe_3O_4@MSN-TPP/PEG-FA). Reproduced with permission [33]. Copyright 2018, Royal Society of Chemistry.

safety and therapeutic effects. In another study, Chen *et al.* developed a kind of metal-phenolic network NP by using DOX and cisplatin together to realize better O_2^- production capacity [31]. The SOD-like activity of polyphenols could further promote the conversion of O_2^- to H_2O_2, resulting in effective tumor inhibition.

Lap, as an *o*-naphthoquinone, has been found to have a lethal effect on cancer cells in the late 20th century [61]. Since then, in-depth research has been carried out and the Lap has been demonstrated to have therapeutic effect on a variety of cancers such as pancreatic cancer, breast cancer and liver cancer [62]. In

the process of studying Lap, its ability to promote the production of H_2O_2 in the presence of NAD(P)H: quinone oxidoreductase-1 (NQO1) was found. This property of Lap can be exploited to develop nanomedicines for CDT [63,64]. Furthermore, this process occurs specifically in cancer cells that overexpress NQO1, which has a protective effect on normal cells. Chen *et al*. developed a pH/ROS dual-responsive nanomedicine (denoted as PtkDOX-NM), which brought new ideas for the combined application of chemotherapy and CDT [34]. In this study, the PtkDOX-NMs were prepared by self-assembly of two types of amphiphilic polymers, pH-responsive PEG-*b*-polydiisopropylaminoethyl methacrylate-*b*-polydopamine (PEG-PDPA-PDA) and ROS-responsive PEG-*b*-polythioketal DOX prodrug (PEG-PtkDOX). Lap and ferric ions were co-loaded in the PtkDOX-NMs. After accumulating in the tumor area through the enhanced permeability and retention (EPR) effect and entering cancer cells, under the influence of the TME acidity, the PtkDOX-NMs were disassembled due to hydrophobic-to-hydrophilic conversion of PDPA segments, so that the loaded contents were quickly released. Then a large amount of H_2O_2 would be produced through Lap catalysis for Fenton reaction and $^{\bullet}OH$ generation. The generated $^{\bullet}OH$ could further cause DOX release by breaking thioketal bonds and thus realize combination therapy (Fig. 6a). The Lap-induced intracellular H_2O_2 production was confirmed by DCFH-DA staining. With the increase of Lap concentration, the ROS level inside NQO1-overespressed A549 cells (Fig. 6b). Cytotoxicity study results showed that the inhibitory effect of nanomedicines without Lap on A549 cells was limited; while the anticancer effect of the nanomedicines was significantly enhanced by addition of Lap (Figs. 6c and d). These results indicated that the Lap-induced H_2O_2 production was the critical process in the cascade of $^{\bullet}OH$ generation and DOX release. Compared with control groups, the Lap-loaded PtkDOX-NMs showed the most potent anticancer effect, indicating combination effect of chemotherapy and CDT. *In vivo* experiments also demonstrated the great effect of PtkDOX-NMs on tumor inhibition (Fig. 6e).

CA is an unsaturated aromatic aldehyde widely present in plants such as cinnamon. It is not only widely used as a flavoring agent in various foods, but also used in the field of medicine due to its antifungal and peripheral blood vessel relaxation effects [65,66]. In addition, at the beginning of the 21st century, the ability of CA to induce cell apoptosis by promoting the production of ROS was discovered [67]. In recent studies, CA-based drug/nanomedicine was developed to amplify oxidative stress by promoting H_2O_2 production and downregulating antioxidant systems, resulting in enhanced tumor cells killing effect [2,36]. By combining with Fenton catalysts, CA has also been used to enhance the efficacy of CDT by increasing the H_2O_2 level. For example, Zhao *et al*. reported a nanoreactor (HA-CD/Fc-CA NP) prepared by host-guest interaction of the bifunctional ferrocene-modified cinnamaldehyde prodrug (Fc-CA) with cyclodextrin-modified hyaluronic acid conjugate (HA-CD) [37]. HA not only improved the biocompatibility and biodegradability of the nanoreactor, but also endowed it with a strong targeting ability for CD44 receptor-overexpressed tumor cells. After cellular internalization, in response to an acidic environment, CA and ferrocene (Fc) will be released due to cleavage of pH-sensitive hydrazone bonds.

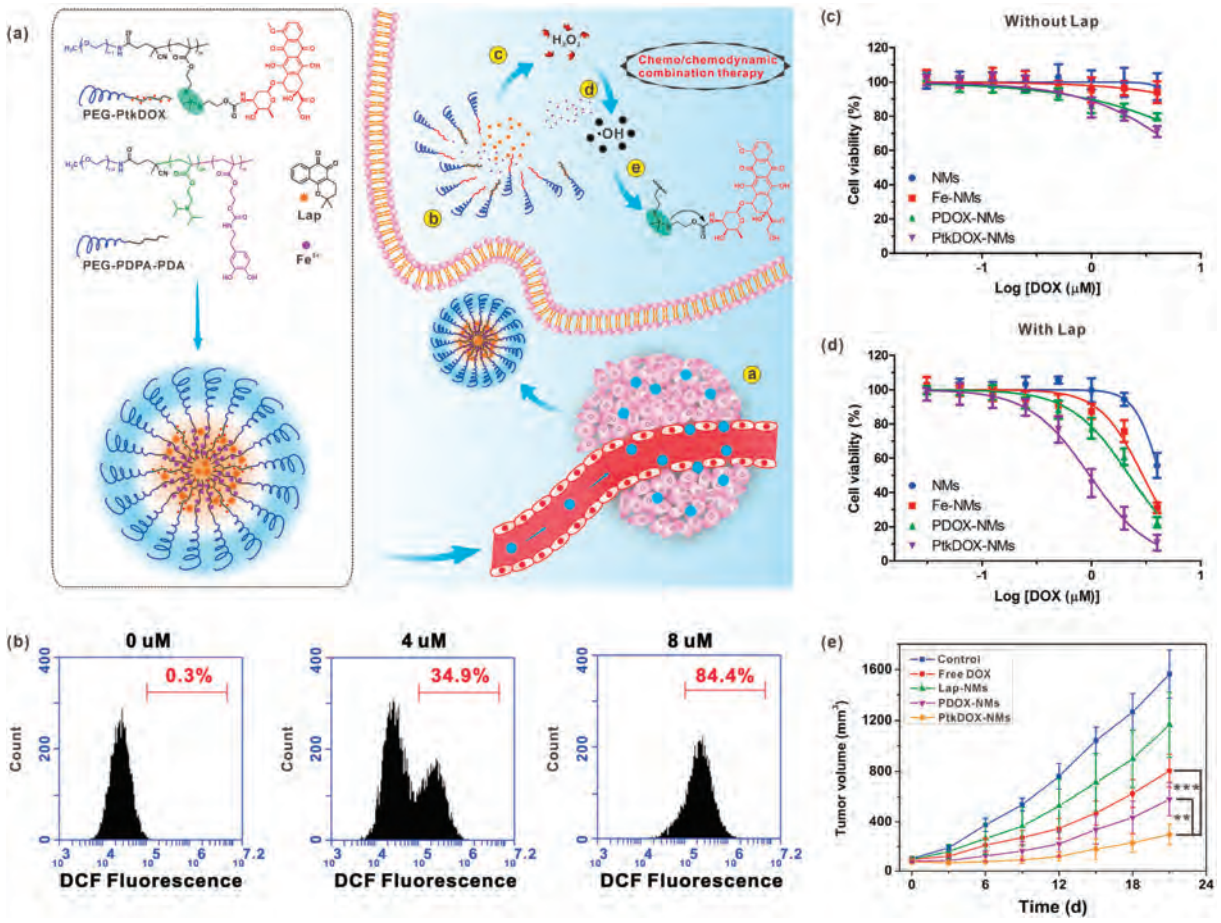

Fig. 6. (a) Schematic illustration of Lap-loaded PtkDOX-NMs for H_2O_2 generation-enhanced chemo/chemodynamic combination therapy. (b) Flow cytometry analysis of DCFH-DA stained A549 cells treated with different concentrations of Lap. Viability of A549 cells incubated with different samples in the absence (c) and presence (d) of Lap. μM: μmol/L. (e) Tumor growth curves of the mice treated with different samples. Reproduced with permission [34]. Copyright 2019, Wiley-VCH.

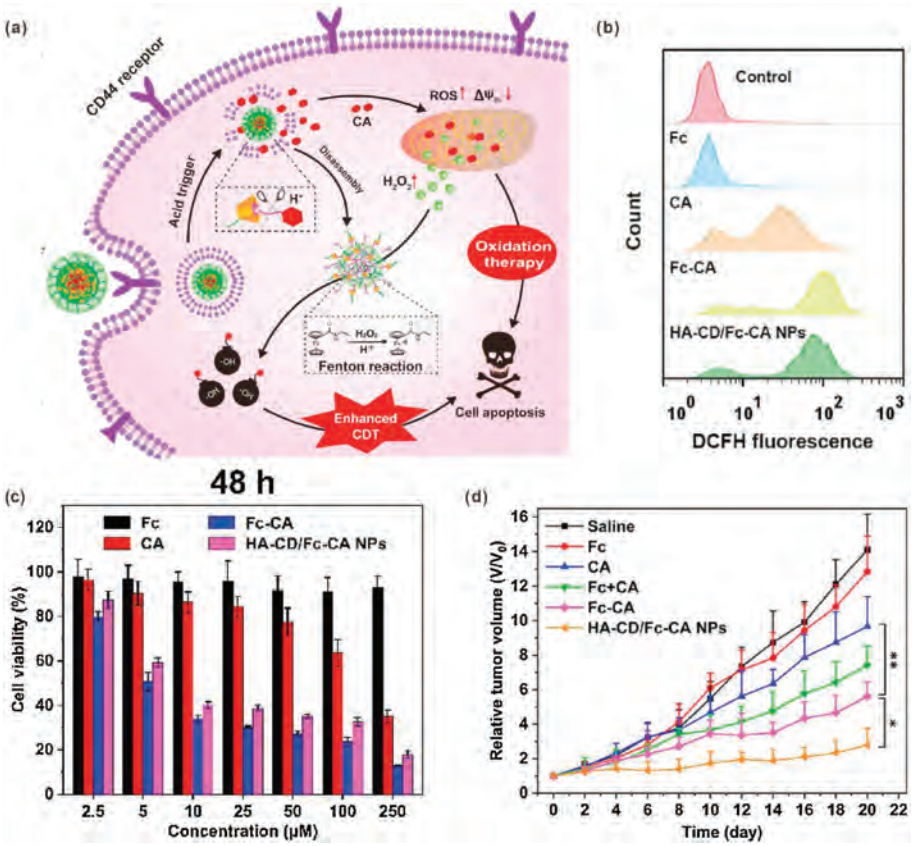

Fig. 7. (a) Schematic illustration of HA-CD/Fc-CA NPs for synergistic chemo/chemodynamic therapy. (b) Flow cytometry analysis of intracellular ROS level in 4T1 cells treated with different formulations. (c) *In vitro* cell cytotoxicity against 4T1 cells of different formulations. μM: μmol/L. (d) Tumor growth curves of the mice treated with different formulations. Reproduced with permission [37]. Copyright 2020, Elsevier.

Attributing to the CA-promoted H_2O_2 generation and Fc-mediated Fenton reaction, highly cytotoxic $^{\bullet}OH$ was generated for enhanced CDT (Fig. 7a). The flow cytometry analysis proved that the intracellular ROS level could be amplified by CA. Compared with free CA, Fc-CA showed better effect, indicated that Fc could convert H_2O_2 into $^{\bullet}OH$ with stronger oxidation capability. The ROS amplification ability of HA-CD/Fc-CA NPs was comparable to that of free Fc-CA (Fig. 7b). The *in vitro* cytotoxicity results proved the anticancer effect of CA-containing groups. Importantly, the HA-CD/Fc-CA NPs showed higher cytotoxicity against 4T1 cells than free CA, indicating Fenton reaction-enhanced therapeutic effect (Fig. 7c). Furthermore, *in vivo* experiments also demonstrated that the HA-CD/Fc-CA NPs had a significant tumor suppressing effect, which was attributed to effective tumor targeting and synergistic chemo/chemodynamic therapy (Fig. 7d).

4. Metal peroxide

Although catalysis strategy is effective, the yield of H_2O_2 is often limited by tumor oxygen level. However, most solid tumors suffer from insufficient oxygen concentration. Therefore, the oxygen-independent H_2O_2 generation strategy will be promising in the treatment of hypoxic tumors. Metal peroxides, which can decompose to produce metal ions and H_2O_2, has attracted more and more attention for developing H_2O_2 self-supplying nanosystems [68].

For example, Dong *et al.* developed a H_2O_2 self-supplying nanosystem for thermal responsive enhanced CDT [39]. To prepare the nanosystem (denoted as Fe-GA/CaO_2@PCM NPs), ultra-small calcium peroxide (CaO_2) NPs and iron-gallic acid NPs (Fe-GA) were encapsulated by organic phase-change materials (PCMs), which can achieve solid-liquid transition through temperature changes. The outer layer of PCM could improve the stability of CaO_2 by isolating it from the outside environment. By changing the ratio of fatty acids or fatty alcohols, the melting point of PCMs can be adjusted to 46 °C [69,70]. Upon 808 nm laser irradiation, the Fe-GA can be used as a photothermal conversion agent to convert light energy into heat, which further induced melting of PCM, leading to rapid release of CaO_2 NPs and Fe-GA. In an acidic intracellular environment, CaO_2 would be decomposed into Ca^{2+} and H_2O_2. Then H_2O_2 would be further converted into $^{\bullet}OH$ through Fe-GA-mediated Fenton reaction, achieving H_2O_2 self-sufficient CDT. In addition, the released Ca^{2+} could induce mitochondrial damage, resulting in synergistic therapy (Fig. 8a). The CaO_2@PCM did not show H_2O_2 generation ability without heating, indicating the protective effect of PCM. However, when CaO_2@PCM was heated to about 50 °C at pH 5.5, a large amount of H_2O_2 was produced, demonstrated that the released CaO_2 NPs were decomposed under acidic condition (Fig. 8b). The H_2O_2 self-sufficient CDT was proved by a methylene blue (MB) assay *in vitro*. As shown in Fig. 8c, in acidic condition with heating, the Fe-GA/CaO_2@PCM NPs could cause significant MB degradation, demonstrating effective $^{\bullet}OH$ generation. Because there was no exogenous H_2O_2, the $^{\bullet}OH$ generation was caused by H_2O_2 self-supplying Fenton reaction. The intracellular ROS detection results demonstrated that the Fe-GA/CaO_2@PCM NPs could significantly improve ROS level under laser irradiation; however, no obvious ROS level improvement was observed in Fe-GA@PCM NPs-treated cells (Fig. 8d). In addition, Ca^{2+} was only detected in cells treated with Fe-GA@PCM NPs and laser irradiation (Fig. 8e), which was consist with the results of ROS detection, indicated that both Ca^{2+} and H_2O_2 came from the decomposition of CaO_2. The mitochondrial membrane potential

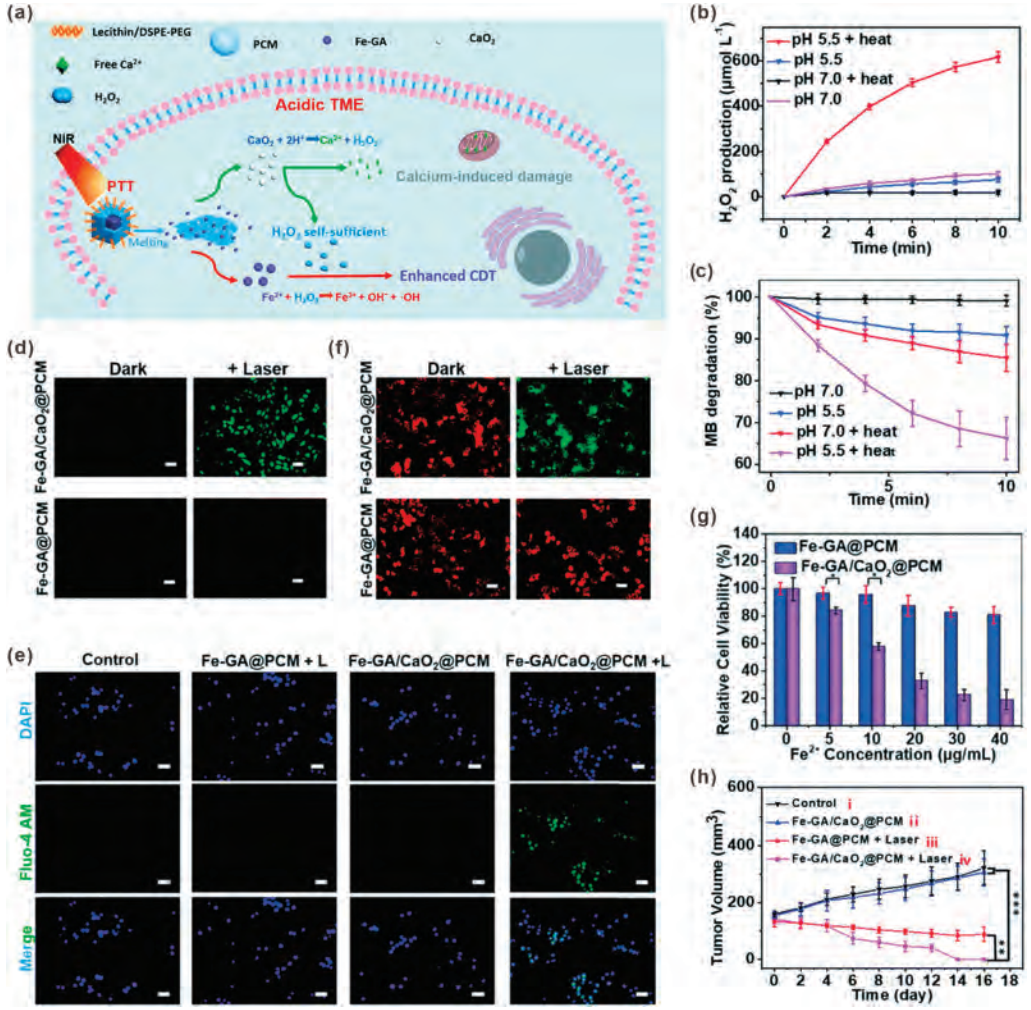

Fig. 8. (a) Schematic illustration of Fe–GA/CaO_2@PCM for H_2O_2 self-sufficient CDT. (b) H_2O_2 production from CaO_2@PCM with different treatments. (c) Fe–GA/CaO_2@PCM NP caused MB degradation under different conditions. Fluorescence images of DCFH-DA probe (d), JC-1 probe (e) and Fluo-4 AM probe (f) stained HeLa cells after different treatments. (g) Viability of HeLa cells incubated with different samples under laser irradiation. (h) Tumor growth curves of the mice treated with different formulations. Reproduced with permission [39]. Copyright 2020, Royal Society of Chemistry.

staining results also proved that only the Fe-GA/CaO_2@PCM NPs with laser irradiation could cause significant mitochondrial damage (Fig. 8f). *In vitro* cell experiments showed that the viability of cells treated with Fe-GA/CaO_2@PCM under laser irradiation was significantly lower than that of Fe-GA@PCM-treated cells, indicating the H_2O_2 self-supplying enhanced CDT (Fig. 8g). *In vivo* antitumor results also proved the efficient tumor inhibition effect of Fe-GA/CaO_2@PCM (Fig. 8h).

In another study, Chen *et al.* developed another metal peroxide, copper peroxide (CP) nanodot, for H_2O_2 self-supplying CDT [40]. In acidic endo/lysosome conditions, CP nanodots would be decomposed into Cu^{2+} and H_2O_2. Compared with other metal peroxides, one major advantage of CP nanodots is that the generated Cu ions can be used as a Fenton catalyst directly. Therefore, both the H_2O_2 and Fenton catalyst were self-supplied simultaneously by CP nanodots without adding other materials, resulting in efficient $^{\bullet}OH$ generation. In addition, the generated $^{\bullet}OH$ would lead to lysosomal lipid peroxidation (LPO) and subsequent release of lysosomal hydrolases to induce cell death (Fig. 9a). It was demonstrated that the CP nanodots were stable in physiological environment (pH 7.4); while rapid decomposed to release Cu^{2+} at pH 5.5 (Fig. 9b). The TMB assay also showed that CP nanodots would decompose under acidic condition to produce a large amount of $^{\bullet}OH$ (Fig. 9c). Based on the H_2O_2 self-supplying property and efficient $^{\bullet}OH$ generation, CP nanodot itself could inhibit tumor cell proliferation. As shown in Figs. 9d and e, the treatment of 20 μg/mL of CP nanodots could lead to more than 80% of U87MG cell death. The CDT-induced LPO was verified by acridine orange (AO) indicator, which emits different fluorescence in different organelles (red: acidic lysosomes; green: cytoplasm and nuclei). As shown in Fig. 9f, in control group, both green and red fluorescence could be detected; however, almost no red fluorescence was detected in U87MG cells treated with CP nanodots, indicated that the lysosomes could be damaged by $^{\bullet}OH$-initiated LPO. Attributing to lysosomal damage, the released lysosomal hydrolases would elicit cancer cell apoptosis.

5. Engineered bacterial bioreactor

By the middle of the nineteenth century, some bacteria such as *Streptococcus pyogenes* have been found to have antitumor effects [71,72]. However, the problems of large individual differences, low repetition rate and high toxicity limited further application of bacterial therapy. In recent years, the rise of synthetic biology has brought new opportunities for bacterial therapy. Synthetic biology refers to the design and construction of artificial biological systems from an engineering perspective [73]. Specifically, for cancer treatment, genetic modification is used to give bacteria certain abilities, or to weaken some of their abilities, thus achieving safe

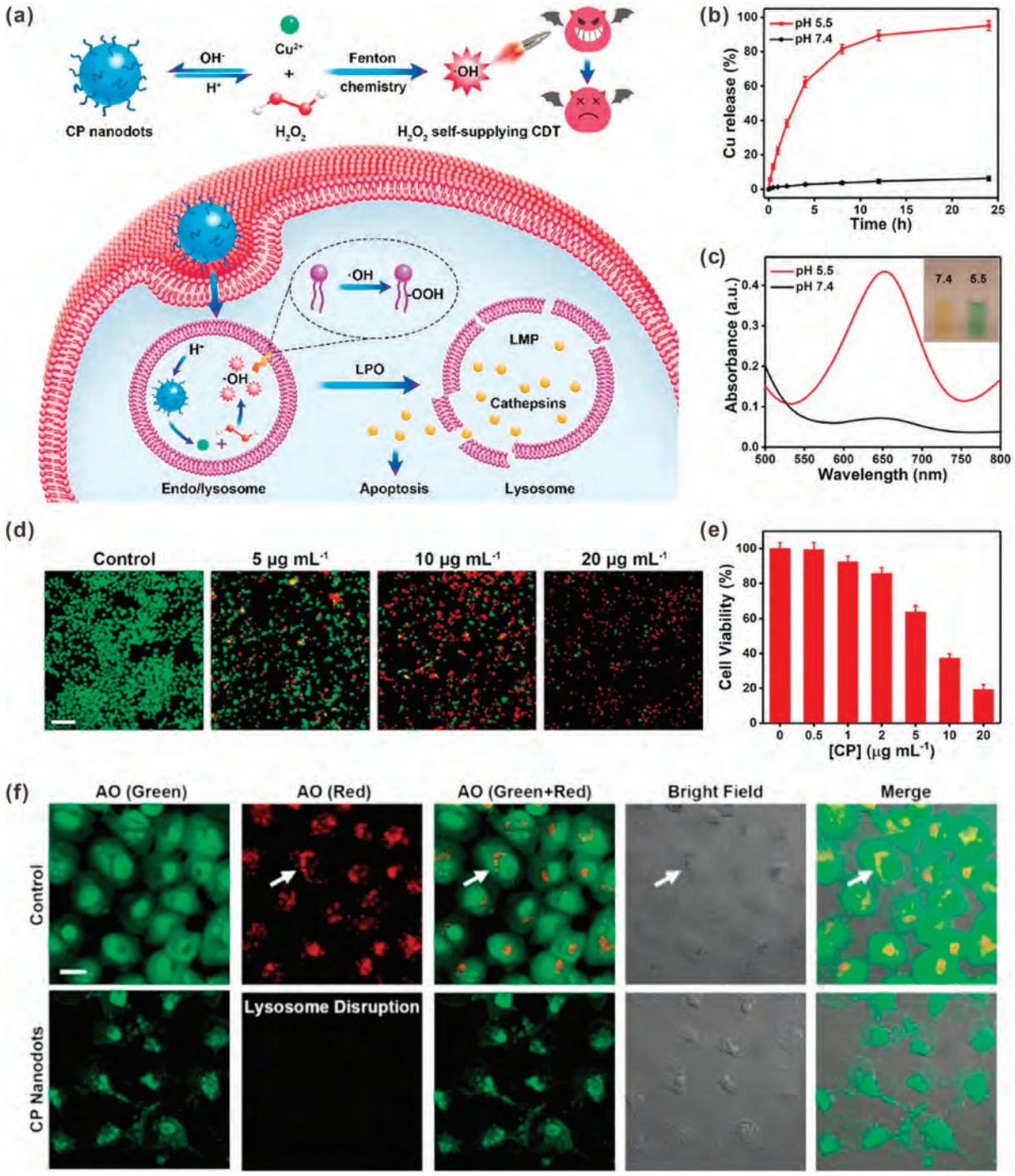

Fig. 9. (a) Schematic illustration of CP nanodots for H_2O_2 self-supplying CDT. (b) *In vitro* Cu release from CP nanodots at pH 7.4 and 5.5. (c) Absorption spectra of TMB incubated with CP nanodots at pH 7.4 and 5.5. (d) Live/dead cell staining results of U87MG cells treated with different concentrations of CP nanodots. (e) Viability of U87MG cells treated with different concentrations of CP nanodots. (f) CLSM images of U87MG cells treated with AO-staining with or without CP nanodots. Reproduced with permission [40]. Copyright 2019, American Chemical Society.

and stable cancer treatment [74]. Recently, Zhang *et al*. reported an integrative bioreactor (Ec-pE@MNP) composed of engineered bacterium and magnetic Fe_3O_4 nanoparticles (MNP) for cancer CDT [42]. In this study, MNP were chemically conjugated on the surface of nonpathogenic bacterium *Escherichia coli* MG1655 (Ec-pE) that overexpresses respiratory chain enzyme II (NDH-2). Due to the tropism of bacteria and the magnetic targeting ability of MNP, the Ec-pE@MNP could effectively accumulate in tumor site. The overexpressed NDH-2 could catalyze the production of H_2O_2 through electrons transfer during bacterial respiration. Afterwards, a Fenton-like reaction occurred under the action of the MNP, generating highly toxic $^{\bullet}OH$ for cancer cell killing (Fig. 10a). Polyacrylamide gel electrophoresis (PAGE) results showed that NDH-2 was expressed by Ec-pE, especially in the presence of isopropyl-β-D-thiogalactoside (IPTG), an inductive agent (Fig. 10b). The intracellular H_2O_2 level was detected by using DCFH-DA. As shown in Fig. 10c, intense fluorescence was found in Ec-pE with IPTG induction group, indicating efficient H_2O_2 generation. In addition, a hydrogen peroxide assay kit was used to measure the H_2O_2 concentrations of media. The result indicated that the

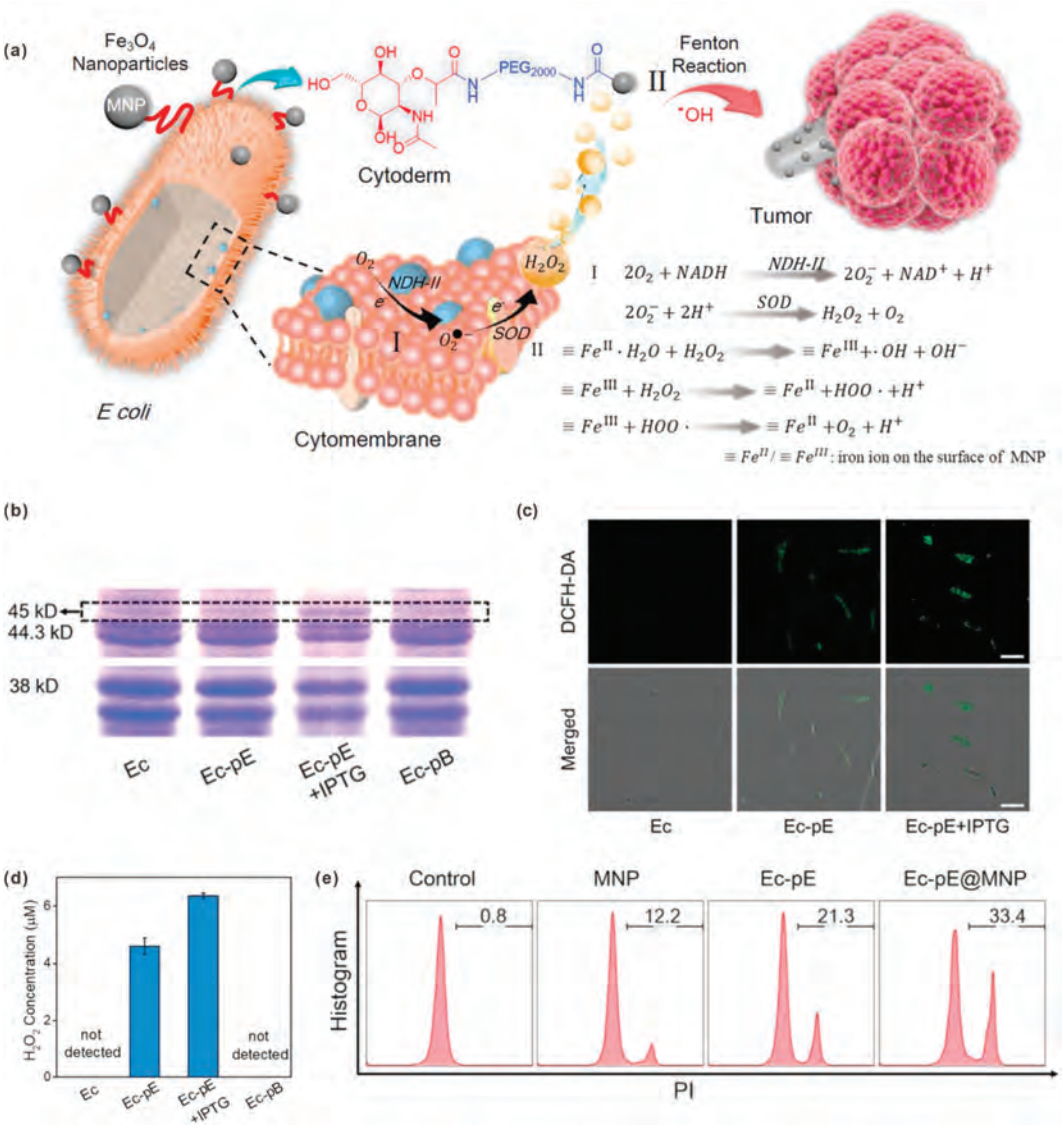

Fig. 10. (a) Schematic illustration of engineered bacterial bioreactor for H_2O_2 production-enhanced CDT. (b) The NDH-2 expression results of different bacteria. (c) CLSM images of different bacteria after DCFH-DA staining. (d) The detection of produced H_2O_2 in different bacteria suspensions (μM: μmol/L). (e) Flow cytometric analysis of PI-stained cells with different treatments. Reproduced with permission [42]. Copyright 2019, Wiley-VCH.

engineered bacterium Ec-pE successfully promoted the production of H_2O_2 (Fig. 10d). In contrast, the amount of H_2O_2 produced by the wild-type strain and the negative control group (Ec-pB) were below the detection limit. According to flow cytometric analysis, the Ec-pE@MNP showed the best effect in inducing cell death (Fig. 10e). In short, this study developed a bacterial-based H_2O_2-generating bioreactor for cancer CDT, and provided new ideas for the future applications of synthetic biology in cancer treatment.

6. Conclusion and perspective

CDT is an emerging cancer treatment approach by exploiting Fenton reaction to convert H_2O_2 into highly toxic $^{\bullet}OH$. In CDT, H_2O_2, as the source of $^{\bullet}OH$, plays very important role in $^{\bullet}OH$ generation efficiency. Although H_2O_2 is overexpressed in tumor microenvironment, the concentration of endogenous H_2O_2 is still at a relatively low level. In order to improve the treatment outcome of CDT, various H_2O_2-generating nanomedicines have been developed in recent years. Through catalysis or self-supply effects, these nanomedicines can promote the H_2O_2 concentration in tumor tissue or cells and thus enhance CDT efficacy.

In this review, we summarized recent advances in H_2O_2-generating nanomedicines that based on enzymes, nanozymes, drugs, metal peroxides and engineered bacteria. Although enhanced CDT was achieved, the H_2O_2-generating strategy still faces some challenges. Firstly, the unsatisfactory biosafety of these nanomedicines is a big problem. For example, GOD and GOD-like nanozymes suffer from high systemic toxicity because the catalytic reaction will also take place in the blood circulation and normal tissues. The inherent toxicity of chemotherapeutic drugs will also exist in drug-mediated CDT process. Secondly, most H_2O_2 generation reactions are depend on tumor oxygen content; however, hypoxia is a typical feature of most solid tumors. Therefore, the efficacy of these nanomedicines in the treatment of hypoxic tumors is limited. Thirdly, although metal peroxides-based self-supply approach is oxygen-independent, the low stability in aqueous environment of metal peroxides may be an obstacle to applications.

For the future work, the following directions need to be taken into consideration: (1) Development of nanomedicines with properties of high tumor targeting efficiency and controlled H_2O_2 production. (2) GSH, as a typical antioxidant overexpressed

in cancer cells, can neutralize ROS and protect cells from oxidative damage; therefore, the combination of H_2O_2 production and GSH depletion would be an effective way to further improve CDT treatment efficiency. (3) Combination of oxygen delivery strategy and H_2O_2-generating agents to attain the sustainable and stable H_2O_2 production. (4) Besides H_2O_2 supply, the Fenton reaction efficiency also affected by other factors such as acidity, slow Fe(III)/Fe(II) conversion, catalyst poisoning. The design of nanomedicines with H_2O_2 production ability and high Fenton reaction efficiency would be a promising direction.

Declaration of competing interest

The authors declare that they have no known competing financial interests or personal relationships that could have appeared to influence the work reported in this paper.

Acknowledgments

This work was supported by the National Natural Science Foundation of China (Nos. 32000991, 51873150), the Young Elite Scientists Sponsorship Program by Tianjin (No. TJSQNTJ-2020-02), the Key project of Tianjin Foundational Research (JingJinJi) Program, China (No. 19JCZDJC64100), the Key Project of Tianjin Nature Science Foundation (No. 16JCZDJC35100), the Tianjin Research Innovation Project for Postgraduate Students (No. 2020YJSB130).

References

[1] J.P. Fruehauf, F.L. Meyskens, Clin. Cancer Res. 13 (2007) 789–794.
[2] J. Noh, B. Kwon, E. Han, et al., Nat. Commun. 6 (2015) 6907.
[3] G. Huang, H. Chen, Y. Dong, et al., Theranostics 3 (2013) 116–126.
[4] B.W. Yang, Y. Chen, J.L. Shi, Chem. Rev. 119 (2019) 4881–4985.
[5] G. Yu, T.Y. Cen, Z. He, et al., Angew. Chem. Int. Ed. 58 (2019) 8799–8803.
[6] S. Wang, R. Tian, X. Zhang, et al., Adv. Mater 33 (2021) 2007488.
[7] S. Wang, G. Yu, W. Yang, et al., Adv. Sci. 8 (2021) 2002927.
[8] Z. He, Y. Dai, X. Li, et al., Small 15 (2019) 1804131.
[9] H. Ranji-Burachaloo, P.A. Gurr, D.E. Dunstan, G.G. Qiao, ACS Nano 12 (2018) 11819–11837.
[10] C. Zhang, W.B. Bu, D.L. Ni, et al., Angew. Chem. Int. Ed. 55 (2016) 2101–2106.
[11] L. Lin, S. Wang, H. Deng, et al., J. Am. Chem. Soc. 142 (2020) 15320–15330.
[12] J. Fang, T. Seki, H. Maeda, Adv. Drug Delivery Rev. 61 (2009) 290–302.
[13] D. Trachootham, J. Alexandre, P. Huang, Nat. Rev. Drug Discovery 8 (2009) 579–591.
[14] Z.M. Tang, Y.Y. Liu, M.Y. He, W.B. Bu, Angew. Chem. Int. Ed. 58 (2019) 946–956.
[15] T.T. Wang, H. Zhang, H.H. Liu, et al., Adv. Funct. Mater. 30 (2020) 1906128.
[16] L.S. Lin, J.B. Song, L. Song, et al., Angew. Chem. Int. Ed. 57 (2018) 4902–4906.
[17] C. Wang, Y.B. Liu, T. Zhou, et al., Chin. Chem. Lett. 30 (2019) 2231–2235.
[18] J. Qu, T. Che, L. Shi, et al., Chin. Chem. Lett. 30 (2019) 1198–1203.
[19] X. Yang, X. Cheng, A.A. Elzatahry, et al., Chin. Chem. Lett. 30 (2019) 324–330.
[20] Y.H. Wang, W. Yin, W.D. Ke, et al., Biomacromolecules 19 (2018) 1990–1998.
[21] Z.M. Tang, H.L. Zhang, Y.Y. Liu, et al., Adv. Mater 29 (2017) 1701683.
[22] Q. Guo, D. Wang, G. Yang, J. Biomed. Nanotechnol. 15 (2019) 2090–2099.
[23] W.P. Li, C.H. Su, Y.C. Chang, et al., ACS Nano 10 (2016) 2017–2027.
[24] M.F. Huo, L.Y. Wang, Y. Chen, J.L. Shi, Nat. Commun. 8 (2017) 357.
[25] J.J. Li, A. Dirisala, Z.S. Ge, et al., Angew. Chem. Int. Ed. 56 (2017) 14025–14030.
[26] C. Fang, Z. Deng, G.D. Cao, et al., Adv. Funct. Mater. 30 (2020) 1910085.
[27] L.L. Feng, R. Xie, C.Q. Wang, et al., ACS Nano 12 (2018) 11000–11012.
[28] S. Gao, H. Lin, H. Zhang, et al., Adv. Sci. 6 (2019) 1801733.
[29] Z.G. Ren, S.C. Sun, R.R. Sun, et al., Adv. Mater 32 (2020) 1906024.
[30] J.J. Liu, M. Wu, Y.T. Pan, et al., Adv. Funct. Mater. 30 (2020) 1908865.
[31] Y.L. Dai, Z. Yang, S.Y. Cheng, et al., Adv. Mater 30 (2018) 1704877.
[32] R.K. Kankala, C.G. Liu, A.Z. Chen, et al., ACS Biomater. Sci. Eng. 3 (2017) 2431–2442.
[33] K. Sun, Z.G. Gao, Y. Zhang, et al., J. Mater. Chem. B Mater. Biol. Med. 6 (2018) 5876–5887.
[34] S. Wang, G.C. Yu, Z.T. Wang, et al., Angew. Chem. Int. Ed. 58 (2019) 14758–14763.
[35] S. Wang, Z. Wang, G. Yu, et al., Adv. Sci. 6 (2019) 1801986.
[36] N.Q. Gong, X.W. Ma, X.X. Ye, et al., Nat. Nanotechnol. 14 (2019) 379–387.
[37] X.Y. Xu, Z.S. Zeng, J. Chen, et al., Chem. Eng. J. 390 (2020) 124628.
[38] M. Zhang, R.X. Song, Y.Y. Liu, et al., Chem 5 (2019) 2171–2182.
[39] S.C. Zhang, C.Y. Cao, X.Y. Lv, et al., Chem. Sci. 11 (2020) 1926–1934.
[40] L.S. Lin, T. Huang, J.B. Song, et al., J. Am. Chem. Soc. 141 (2019) 9937–9945.
[41] L.S. Lin, J.F. Wang, J.B. Song, et al., Theranostics 9 (2019) 7200–7209.
[42] J.X. Fan, M.Y. Peng, H. Wang, et al., Adv. Mater 31 (2019) 1808278.
[43] W. Fan, N. Lu, P. Huang, et al., Angew. Chem. Int. Ed. 56 (2017) 1229–1233.
[44] M. Wang, D.M. Wang, Q. Chen, et al., Small 15 (2019) 1903895.
[45] J.J. Li, Y.F. Li, Y.H. Wang, et al., Nano Lett. 17 (2017) 6983–6990.
[46] H. Wei, E.K. Wang, Chem. Soc. Rev. 42 (2013) 6060–6093.
[47] M. Comotti, C. Della Pina, R. Matarrese, M. Rossi, Angew. Chem. Int. Ed. 43 (2004) 5812–5815.
[48] J.N. Li, W.Q. Liu, X.C. Wu, X.F. Gao, Biomaterials 48 (2015) 37–44.
[49] D. Hu, L. Chen, Y. Qu, et al., Theranostics 8 (2018) 1558–1574.
[50] Y.J. Sang, F.F. Cao, W. Li, et al., J. Am. Chem. Soc. 142 (2020) 5177–5183.
[51] S. Ghosh, Bioorg. Chem. 88 (2019) 102925.
[52] A. Brozovic, A. Ambriovic-Ristov, M. Osmak, Crit. Rev. Toxicol. 40 (2010) 347–359.
[53] H.J. Kim, J.H. Lee, S.J. Kim, et al., J. Neurosci. 30 (2010) 3933–3946.
[54] M. Ushio-Fukai, Y. Nakamura, Cancer Lett. 266 (2008) 37–52.
[55] S.T. Duggan, G.M. Keating, Drugs 71 (2011) 2531–2558.
[56] D.D. Von Hoff, M.W. Layard, P. Basa, et al., Ann. Intern. Med. 91 (1979) 710–717.
[57] X. Zhang, S. Wang, G. Cheng, et al., Matter 4 (2021) 26–53.
[58] S.D. Kan, W.M. Cheung, Y.L. Zhou, W.S. Ho, Planta Med. 80 (2014) 70–76.
[59] M. Gilleron, X. Marechal, D. Montaigne, et al., Biochem. Biophys. Res. Commun. 388 (2009) 727–731.
[60] W.P. Tsang, S.P.Y. Chau, S.K. Kong, et al., Life Sci. 73 (2003) 2047–2058.
[61] A.B. Pardee, Y.Z. Li, C.J. Li, Curr. Cancer Drug Targets 2 (2002) 227–242.
[62] D.C. Ferraz da Costa, L. Pereira Rangel, M. Martins-Dinis, et al., Molecules 25 (2020) 893.
[63] X. Ma, X. Huang, G. Huang, et al., Adv. Healthcare Mater 3 (2014) 1210–1216.
[64] E. Blanco, E.A. Bey, C. Khemtong, et al., Cancer Res. 70 (2010) 3896–3904.
[65] T.C. Huang, Y.L. Chung, M.L. Wu, S.M. Chuang, J. Agric. Food Chem. 59 (2011) 5164–5171.
[66] W. Yoo, D. Yoo, E. Hong, et al., J. Control. Release 269 (2018) 235–244.
[67] H. Ka, H.J. Park, H.J. Jung, et al., Cancer Lett. 196 (2003) 143–152.
[68] C.C. Huang, W.T. Chia, M.F. Chung, et al., J. Am. Chem. Soc. 138 (2016) 5222–5225.
[69] Q. Li, L.H. Sun, M.M. Hou, et al., ACS Appl. Mater. Interfaces 11 (2019) 417–429.
[70] Y.N. Dai, J.Z. Su, K. Wu, et al., ACS Appl. Mater. Interfaces 11 (2019) 10540–10553.
[71] J.M. Pawelek, K.B. Low, D. Bermudes, Lancet Oncol. 4 (2003) 548–556.
[72] W.B. Coley, Ann. Surg. 14 (1891) 199–220.
[73] D.E. Cameron, C.J. Bashor, J.J. Collins, Nat. Rev. Microbiol. 12 (2014) 381–390.
[74] P.N.L. Vo, H.M. Lee, D. Na, J. Microbiol. Biotechnol. 29 (2019) 845–855.